Pakistan Veterinary Journal

ISSN: 0253-8318 (PRINT), 2074-7764 (ONLINE)
DOI: 10.29261/pakvetj/2026.248

RESEARCH ARTICLE

Senkyunolide A Relieves Mammary Inflammatory Damage Through Suppressing Inflammasome-Dependent Pyroptosis and Balancing Mitophagy

Mingfeng Ji[1,a], Ji Chen[1,a], Yumeng Fu[1,a], Qixuan He[1], Jiatong Sui[1], Wenying Bi[1], Feiyan Dai[1], Xiaolong Gu[1], Mahmoud Kandeel[2], Shiqi Dong[3*] and Weijie Qu[1*]

[1]The Yunnan Key Laboratory of Veterinary Etiological Biology, College of Veterinary Medicine, Yunnan Agricultural University, Kunming 650201, China; [2]Department of Biomedical Sciences, College of Veterinary Medicine, King Faisal University, 31982 Al-Ahsa, Saudi Arabia; [3]College of Animal Science and Technology, Tarim University, Aral 843300, China. [a]These authors contributed equally to this article.
*Corresponding author: tcvm@taru.edu.cn (SD); 1401075010@qq.com (WQ)

ARTICLE HISTORY (26-1154)

Received: September 26, 2026
Revised: October 24, 2026
Accepted: October 27, 2026
Published online: October 30, 2026

Key words:
Mammary epithelial barrier
Mastitis
Mitophagy
Pyroptosis
Senkyunolide A

ABSTRACT

Mastitis leads to mammary lesions driven by severe inflammation, oxidative stress and disrupted epithelial barriers. Senkyunolide A (SenA), an active phthalide from Ligusticum chuanxiong, possesses anti-inflammatory activity, but its mechanism against mastitis remains undefined. We investigated SenA's protective effects via inflammatory mammary injury models and HC11 mammary epithelial cells challenged with H_2O_2. Transcriptomic and proteomic screening pinpointed disturbed pyroptosis and mitophagy pathways in inflamed mammary tissue to guide mechanistic assays. In inflammatory mammary tissue, SenA at two dosages alleviated oedema, suppressed pro-inflammatory cytokines and oxidative indicators, boosted anti-inflammatory and antioxidant levels, and recovered intact breast acini morphology. SenA blocked NLRP3 inflammasome-triggered pyroptosis, regulated PINK1/Parkin-dependent mitophagy, and upregulated ZO-1, occludin and claudin-3 to restore epithelial barrier integrity. In epithelial cells, SenA dose-dependently reduced H_2O_2 induced cell leakage and pyroptosis. In summary, SenA alleviates mammary inflammatory damage through synergistic modulation of mitophagy, inflammasome-mediated pyroptosis and epithelial barrier function.

To Cite This Article: Ji M, Chen J, Fu Y, He Q, Sui J, Bi W, Dai F, Gu X, Kandeel M, Dong S and Qu W, 2026. Senkyunolide a relieves mammary inflammatory damage through suppressing inflammasome-dependent pyroptosis and balancing mitophagy. Pak Vet J, 46(10): 2591-2600. http://dx.doi.org/10.29261/pakvetj/2026.248

INTRODUCTION

Mastitis is a common inflammatory disease of the mammary gland during lactation. It is characterized by mammary swelling, epithelial injury, inflammatory cell infiltration and impaired tissue function (Bao *et al*., 2023; Luo *et al*., 2023). Although infection, milk stasis and local stress can initiate mastitis, the severity of tissue damage is largely influenced by the magnitude and persistence of the inflammatory response (Xiong *et al*., 2024; Chen *et al*., 2025). Excessive cytokine production, oxidative stress and disruption of the epithelial barrier can amplify mammary injury and delay tissue recovery (Suzuki *et al*., 2021).

As a dominant disorder in dairy livestock, mastitis imposes staggering economic losses on global animal husbandry sectors, driven by diminished milk yield, discarded contaminated milk, extra veterinary expenditures and premature elimination of chronically diseased individuals (Aghamohammadi *et al*., 2018; Gonçalves *et al*., 2022; Yang *et al*., 2025). Clinical cases present with red, swollen udder parenchyma and abnormal milk texture (Zhang *et al*., 2023), while subclinical mastitis lacks overt visible signs yet elevates somatic cell counts and deteriorates milk processing performance (Watanabe *et al*., 2025). Conventional antibiotic interventions for farm mastitis further raise concerns about antimicrobial resistance and residual pollutants in dairy products, creating an urgent demand for safe, multi target natural alternative therapeutics.

Natural products remain an important source of anti-inflammatory and immunomodulatory compounds (Biswas *et al*., 2023; Zhou *et al*., 2023). Ligusticum chuanxiong Hort. is a traditional medicinal herb widely used in East Asia, and phthalides are considered among its major bioactive constituents. Senkyunolide A (SenA) is one of the representative phthalide compounds isolated from L.

chuanxiong. Previous studies have suggested that SenA and related phthalides exert anti-inflammatory, antioxidant and cytoprotective effects in different disease models. In clinical practice, herbal preparations containing anti-inflammatory botanical constituents have also been used as complementary approaches for inflammatory conditions(Sneha Sri *et al*., 2025). However, whether SenA protects against mastitis and how it acts on inflammatory mammary injury remain insufficiently understood.

Mammary epithelium supports milk synthesis while serving as a frontline innate immune barrier (Xu *et al*., 2022). Tight junction proteins including ZO-1, occludin and claudins physically segregate mammary gland luminal and interstitial spaces; breakdown of this compartmentalization enables unrestricted diffusion of proinflammatory mediators across mammary tissue, exacerbating mastitic lesions (Hu *et al*., 2024). Therefore, preservation of mammary epithelial barrier integrity is an important part of controlling mastitis associated tissue damage.

NLRP3 inflammasome signaling drives inflammatory tissue damage by detecting cellular danger cues to trigger caspase-1 cleavage, IL-1β maturation and GSDMD proteolysis (Downs *et al*., 2020). Truncated GSDMD-N inserts into cell membranes to form pores, triggering pyroptosis and amplifying local inflammatory cascades, this cycle worsens epithelial barrier leakage and immune dysregulation within inflamed mammary tissue (Shao *et al*., 2022).

Mitochondrial dysfunction acts as an upstream trigger linking oxidative stress to NLRP3 hyperactivation. Injured mitochondria overproduce reactive oxygen species and release damage associated molecular patterns that prime inflammasome assembly (Xiao *et al*., 2025). Mitophagy, a conserved mitochondrial quality surveillance pathway mediated by the autophagy lysosome axis, eliminates impaired mitochondria to dampen these pro-inflammatory mitochondrial signals. Prior work confirms mitophagic flux limits aberrant NLRP3 activation, implying mitochondrial homeostasis shapes the progression of inflammatory mammary injury.

Based on these considerations, we investigated whether SenA protects against LPS induced murine mastitis by modulating mitophagy related mitochondrial quality control, reducing inflammasome dependent pyroptotic injury and preserving mammary epithelial barrier integrity (Wu *et al*., 2025). An H_2O_2 induced injury model in HC11 mouse mammary epithelial cells was further used to evaluate the epithelial response under oxidative stress. By integrating transcriptomic and proteomic analyses with inflammatory, oxidative stress, pyroptosis related, mitophagy related and tight junction protein assays, we aimed to clarify the immunopharmacological action of SenA in mastitis.

MATERIALS AND METHODS

Animals and ethical approval: The eight-week-old female mice used in the study were obtained from SPF Biotechnology Co., Ltd. (Beijing, China). All mice were kept in a clean environment with free access to food and water. The animals were treated in accordance with the rules of the institution for the care and use of animals in experiments. All animal experiments were approved by the Animal Ethics Committee of Yunnan Agricultural University (approval No. APYNAU20260730).

LPS induced murine mastitis model and dosing regimen: Following parturition, lactating mice were allocated randomly into five experimental groups (n = 8 per group): normal control (NC), model control (MC), meloxicam-treated positive control (PC), low-dose SenA (SenA L), and high-dose SenA (SenA H).

Senkyunolide A was purchased from MedChemExpress (Cat. No. HY-N0743; purity, 99.32%). For animal administration, SenA was dissolved in dimethyl sulfoxide and diluted with normal saline before use. From day 7 after parturition, mice in the SenA treated groups received SenA by intragastric gavage once daily at doses of 20 or 40mg/kg. Meloxicam was purchased from MedChemExpress (Cat. No. HY-B0261) and used as the positive control drug. The PC group received meloxicam at 5mg/kg by gavage. Mice in the NC and MC groups received the same volume of vehicle.

To establish the mastitis model, mice were anaesthetized with isoflurane. Lipopolysaccharide (Solarbio, Cat. No. L8880) was dissolved in sterile water for injection to prepare a working solution at 0.2mg/mL. A volume of 50μL LPS solution was infused into the fourth mammary gland via the teat duct for each animal. Animals assigned to the NC group received an equivalent volume of sterile vehicle instead. Twenty-four hours post LPS challenge, mice were humanely euthanized by carbon-dioxide inhalation. Blood and mammary gland tissues were then harvested for subsequent laboratory analyses.

Cell culture and H_2O_2 induced injury model: HC11 mouse mammary epithelial cells were cultured in RPMI-1640 medium supplemented with 10% fetal bovine serum and 1% penicillin-streptomycin. Cells were incubated at 37°C in a humidified atmosphere containing 5% CO_2.

For the oxidative injury model, HC11 cells were divided into four groups: control group, H_2O_2 group, H_2O_2 and SenA 25μM group and H_2O_2 and SenA 50μM group. SenA was prepared from the same stock compound described above. Hydrogen peroxide was freshly prepared in culture medium before treatment. Cells were pretreated with SenA at 25 or 50μM for 24h and then exposed to 800μM H_2O_2 for 24 h. After treatment, culture supernatants were collected for LDH analysis, and cells were harvested for ATP measurement and western blotting.

ATP levels and LDH release were measured using commercial kits from Beijing Solarbio Science & Technology Co., Ltd. The catalogue numbers were BC0305 for ATP and BC0685 for LDH. Assays were performed according to the manufacturer's protocols.

Breast index: Following humane euthanasia of experimental mice by carbon-dioxide inhalation, target mammary gland tissues were surgically excised, with surrounding adipose and connective tissue thoroughly trimmed away to avoid weight measurement bias. Individual mammary tissue wet weight and corresponding

whole-body body weight of each mouse were recorded using a high-precision electronic balance. The breast index, an indicator reflecting mammary gland oedema and inflammatory swelling, was calculated using the following formula:

Breast index = mammary gland weight / body weight × 100%

ELISA and biochemical assays: Upon humane euthanasia of mice, whole-blood specimens were promptly collected. Blood samples were incubated at room temperature for 30 min to permit complete coagulation, followed by centrifugation at 3 000 × g for 15 min at 4 °C to separate serum from blood clots. The resulting serum supernatants were carefully aliquoted into cryovials and stored at −80 °C to avoid repeated freeze-thaw cycles prior to cytokine measurement. Serum concentrations of IL-1β, IL-6 and IL-10 were quantified using ELISA kits from Hangzhou Lianke Biotechnology Co., Ltd (catalogue numbers: EK201B, EK206 and EK210). All assay steps were carried out in full accordance with the manufacturer-supplied instructions.

Collected mammary tissues were immediately transferred into ice-cold homogenization buffer and homogenized on ice with a high-speed tissue homogenizer to prevent protein degradation. The resulting tissue homogenates were centrifuged at 12 000 × g for 15 min at 4°C. Following centrifugation, the upper clear supernatants were cautiously collected, avoiding disturbance of the sediment pellet, and subjected to subsequent biochemical assays for MPO activity, MDA content, GSH level and CAT activity. These biochemical indicators were measured using commercial assay kits from Beijing Solarbio Science & Technology Co., Ltd. The catalogue numbers were BC5715, BC6410, BC1175 and BC0205, respectively. All assays were performed under identical experimental conditions across all experimental groups.

Histological analysis: Excised mammary tissue samples were immediately immersed in 4% paraformaldehyde for adequate tissue fixation. Following fixation, samples underwent sequential gradient ethanol dehydration, xylene clearing, and paraffin infiltration for paraffin embedding. Embedded tissue blocks were cut into 5 μm-thick sections using a rotary microtome. Sections were subjected to standard hematoxylin and eosin (H&E) staining procedures. Stained slices were visualized under an optical light microscope to assess histopathological lesions, including mammary oedema, inflammatory cell infiltration, alveolar collapse and glandular architectural disruption. Representative images from each group were acquired for comparative histopathological evaluation.

Immunofluorescence staining: Paraffin embedded mammary tissue sections were de-waxed and rehydrated before antigen retrieval. Following permeabilization and blocking steps, sections were incubated overnight at 4 °C with primary antibodies targeting NLRP3, LC3B, TOM20, ZO-1, occludin and claudin-3 (Table 1).

After thorough washing, tissue sections were probed with fluorophore-labelled secondary antibodies and counter-stained with DAPI. Micrographs were acquired using identical instrument parameters across all samples and ImageJ software was used to quantify fluorescence intensity.

Table 1: Antibody Names and Sources

Antibody	Supplier	Catalogue No.
NLRP3	Cell Signaling Technology	15101
IL-1β	Cell Signaling Technology	12242
Caspase-1	Cell Signaling Technology	24232
Cleaved caspase-1	Cell Signaling Technology	89332
GSDMD-F	Cell Signaling Technology	39754
GSDMD-N	Cell Signaling Technology	10137
PINK1	Cell Signaling Technology	89010
Parkin	Cell Signaling Technology	2132
P62	Cell Signaling Technology	5114
LC3A/B	Cell Signaling Technology	12741
LC3B	Cell Signaling Technology	83506
TOM20	Cell Signaling Technology	42406
ZO-1	Proteintech	21773-1-AP
Occludin	Proteintech	27260-1-AP
Claudin-3	Proteintech	16456-1-AP
β-actin	Proteintech	66009-1-Ig
HRP-Goat Anti-Rabbit IgG Secondary Antibody	Proteintech	RGAR301
HRP-Goat Anti-Mouse IgG Secondary Antibody	Proteintech	RGAM001
Plus 488-Goat Anti-Rabbit Secondary Antibody	Proteintech	RGAR002
Plus 594-Goat Anti-Rabbit Secondary Antibody	Proteintech	RGAR004
Plus 488 -Goat Anti-Mouse Secondary Antibody	Proteintech	RGAM002

Western blotting: We lysed mammary tissues or HC11 cells in RIPA buffer with protease inhibitors, then measured protein concentrations using a BCA assay. We loaded equal amounts of protein onto SDS–PAGE gels, transferred them to PVDF membranes, blocked the membranes and incubated them overnight at 4°C with the primary antibodies listed in the figure legends (Table 1).

Following the process of washing, the membranes were then subjected to an incubation with HRP-conjugated secondary antibodies. The visualization of protein bands was achieved through the utilization of enhanced chemiluminescence, while the quantification process was conducted by employing the ImageJ software. The β-actin was employed as the loading control.

Transcriptomic and proteomic analyses: Mammary tissue samples from the NC and MC groups were used for transcriptomic and proteomic analyses. Each group contained six biological replicates. Transcriptomic and proteomic analyses were performed by Shanghai Majorbio Bio-pharm Technology Co., Ltd.

Differential genes and proteins were screened with the thresholds of $|\log_2 FC| > 1$ and adjusted P-value < 0.05. GO and KEGG enrichment analyses were then carried out to uncover biological processes and signaling pathways linked to LPS-provoked mammary inflammatory injury.

Statistical analysis: Data are shown as mean±SEM. We ran all statistical analyses in GraphPad Prism 11. For comparisons across three or more groups, we used one-way ANOVA with a post-hoc test for multiple comparisons. Bars sharing the same lowercase letter aren't significantly different from each other—those with different letters are. We considered $P<0.05$ statistically significant.

RESULTS

Multi omics analysis reveals inflammatory cell death and mitophagy related changes in LPS induced murine mastitis: Transcriptomic analysis was first performed to characterize gene expression changes in mammary tissues from the MC and NC groups. Compared with the NC group, the MC group showed 5,586 upregulated and 6,688 downregulated genes (Fig. 1A). Among the differentially expressed genes, IL-1β, NLRP3, GSDMD and caspase-1 were highlighted, suggesting that genes associated with inflammatory injury and regulated cell death were markedly altered after LPS challenge. GO enrichment analysis showed that the differentially expressed genes were mainly associated with NADP binding, MAP kinase serine/threonine phosphatase activity, xenobiotic metabolic process, regulation of the pentose phosphate shunt and NADPH oxidation (Fig. 1B). KEGG analysis showed enrichment of phagosome, metabolism of xenobiotics by cytochrome P450, efferocytosis, mTOR signaling pathway and PI3K–Akt signaling pathway (Fig. 1C).

Proteomic analysis was further performed to examine whether related alterations were also present at the protein level. In the MC group, 3,979 proteins were upregulated and 1,712 proteins were downregulated compared with the NC group (Fig. 1D). NLRP3, GSDMD, IL-1β and caspase-1 were among the altered proteins. GO enrichment analysis showed that these proteins were mainly involved in autophagy, regulation of autophagy, macroautophagy, autophagosome assembly, programmed cell death, cell death, autophagosome organization and autophagosome membrane (Fig. 1E). KEGG analysis further showed enrichment of autophagy, NOD-like receptor signaling pathway, apoptosis, necroptosis, IL-17 signaling pathway, mitophagy and PI3K–Akt signaling pathway (Fig. 1F).

SenA alleviates mammary inflammatory injury and oxidative stress in LPS induced murine mastitis: The in vivo experimental design is shown in Fig. 2A. After LPS challenge, the MC group showed a significant increase in breast index compared with the NC group. SenA treatment reduced the breast index, and the reduction was more evident in the SenA H group (Fig. 2B, $P<0.05$).

Serum cytokine analysis showed that IL-1β and IL-6 were increased in the MC group. Treatment with meloxicam, SenA L or SenA H reduced both cytokines compared with the MC group (Fig. 2C and D, $P<0.05$). In contrast, IL-10 was decreased after LPS challenge and was restored after meloxicam or SenA treatment (Fig. 2E, $P<0.05$).

Inflammatory and oxidative stress related indices were then examined in mammary tissue. MPO activity and MDA content were increased in the MC group, whereas SenA treatment reduced both indices, especially at the high dose (Fig. 2F and G, $P<0.05$). GSH and CAT levels were decreased by LPS and were increased after SenA treatment to varying degrees (Fig. 2H and I, $P<0.05$). H&E staining showed inflammatory cell infiltration, alveolar compression and disorganized mammary structure in the MC group. These pathological changes were attenuated after SenA treatment, with the most obvious improvement observed in the SenA H group (Fig. 2J).

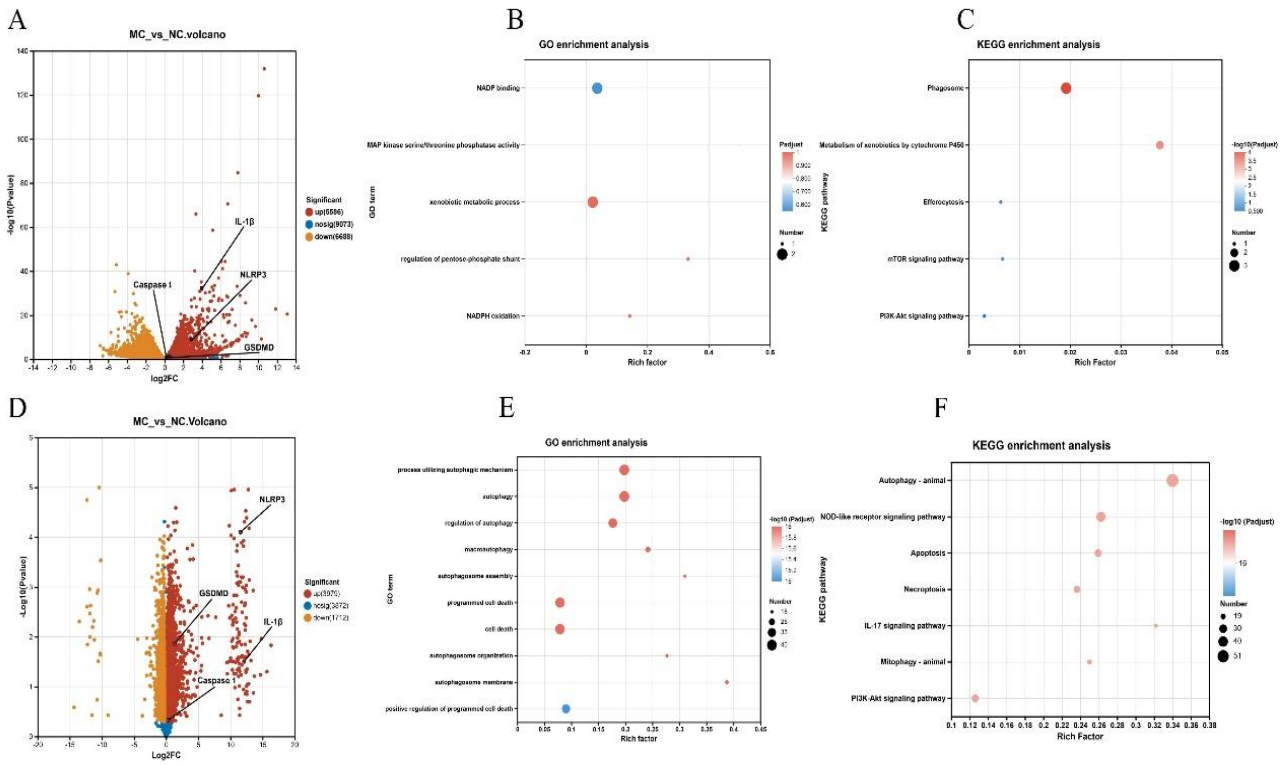


Fig. 1: Multi-omics analysis reveals molecular alterations in LPS-induced murine mastitis. A–C, Transcriptomic analysis of mammary tissues from NC and MC mice. A, Volcano plot showing differentially expressed genes, with representative inflammation- and cell death-related genes indicated. B, GO enrichment analysis of differentially expressed genes. C, KEGG enrichment analysis of differentially expressed genes. D–F, Proteomic analysis of mammary tissues from NC and MC mice. D, Volcano plot showing differentially expressed proteins, with representative inflammasome- and pyroptosis-related proteins indicated. E, GO enrichment analysis of differentially expressed proteins. F, KEGG enrichment analysis of differentially expressed proteins.

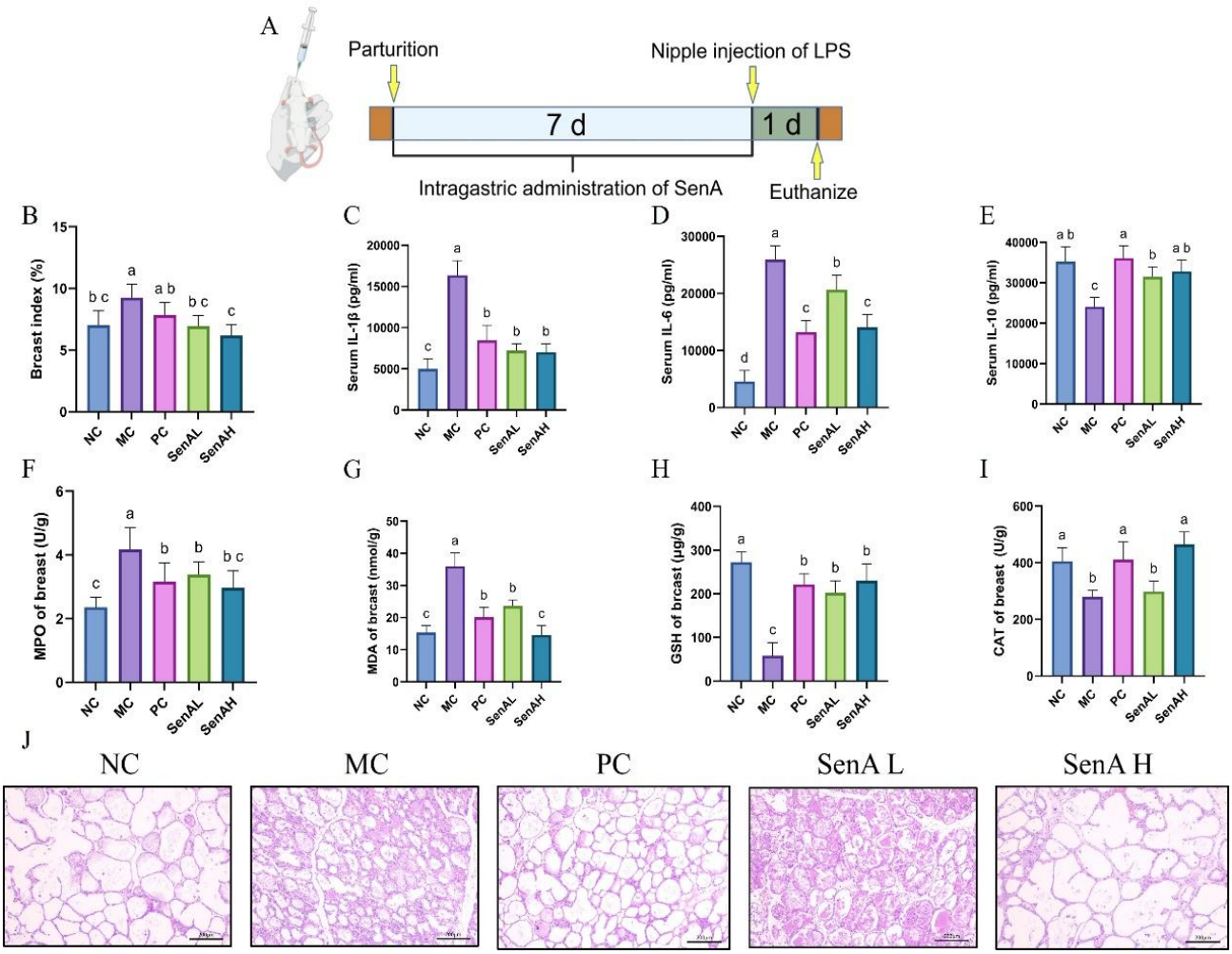


Fig. 2: SenA alleviates mammary inflammatory injury and oxidative stress in LPS-induced murine mastitis. A, Experimental design. Lactating mice received SenA by gavage from day 7 after parturition, followed by intramammary injection of 50 μl LPS solution at 0.2 mg/ml into the fourth mammary gland. Samples were collected 24 h after LPS challenge. B, Breast index. C–E, Serum IL-1β, IL-6 and IL-10 levels. F–I, Mammary MPO, MDA, GSH and CAT levels. J, Representative H&E-stained mammary tissue sections from NC, MC, PC, SenA L and SenA H groups.

SenA reduces pyroptosis related protein processing and alters mitophagy related responses in mammary tissue: Based on the multi omics results, NLRP3 and pyroptosis related proteins were further examined. Immunofluorescence staining showed weak NLRP3 fluorescence in the NC group, whereas the MC group displayed stronger NLRP3 signal (Fig. 3A). Quantitative analysis confirmed that NLRP3 fluorescence intensity was increased after LPS challenge. Meloxicam and SenA treatment reduced NLRP3 fluorescence, with a greater reduction in the SenA H group than in the SenA L group (Fig. 3B, $P<0.05$).LC3II and TOM20 staining was used to observe mitophagy related changes. LC3II/TOM20 associated fluorescence differed among groups, and the SenA H group showed an obvious increase in the merged signal (Fig. 3C and D).

Western blotting further showed that NLRP3 expression was increased in the MC group and reduced after meloxicam or SenA treatment (Fig. 3E and F, $P<0.05$). Mature IL-1β was also elevated in the MC group and decreased after treatment (Fig. 3H, $P<0.05$). Total caspase-1 showed group dependent variation, whereas cleaved caspase-1 was reduced by meloxicam and SenA, with the lowest level in the SenA H group (Fig. 3I and J, $P<0.05$). GSDMD-N was increased in the MC group and decreased after meloxicam or SenA treatment (Fig. 3L, $P<0.05$).

Mitophagy related proteins were also detected. PINK1 and Parkin were increased in the MC group. SenA H reduced both proteins, and PINK1 showed the lowest expression in the SenA H group (Fig. 3M–O, $P<0.05$). P62 was decreased in the MC group and increased after SenA H treatment (Fig. 3P, $P<0.05$). LC3 I was increased by LPS and reduced after treatment, whereas LC3 II was increased in the MC group and further changed after meloxicam or SenA treatment (Fig. 3Q and R, $P<0.05$). These data showed that SenA treatment was accompanied by reduced pyroptosis related protein processing and altered mitophagy related protein expression in mammary tissue.

SenA restores tight junction proteins in LPS induced murine mastitis: To evaluate mammary epithelial barrier integrity, ZO-1, ccludin and claudin-3 were examined by immunofluorescence staining and western blotting. ZO-1 fluorescence was strong and relatively continuous in the NC group but markedly weakened in the MC group (Fig. 4A). Meloxicam and SenA treatment restored ZO-1 fluorescence to different extents, with stronger recovery in the SenA H group than in the SenA L group (Fig. 4B, $P<0.05$).

Occludin staining showed a similar pattern. The MC group displayed weak occludin fluorescence, whereas meloxicam and SenA H treatment partially restored the signal (Fig. 4C and D). Claudin-3 fluorescence was also decreased after LPS challenge and increased after meloxicam or SenA treatment. SenA H showed a stronger restorative effect than SenA L (Fig. 4E and F, $P<0.05$).

Western blotting confirmed these changes. ZO-1, occludin and claudin-3 were decreased in the MC group. Meloxicam and SenA H increased the expression of these tight junction proteins, while the effect of SenA L was relatively weaker (Fig. 4G–J, $P<0.05$). These results suggested that SenA helped preserve mammary epithelial barrier integrity under inflammatory conditions.

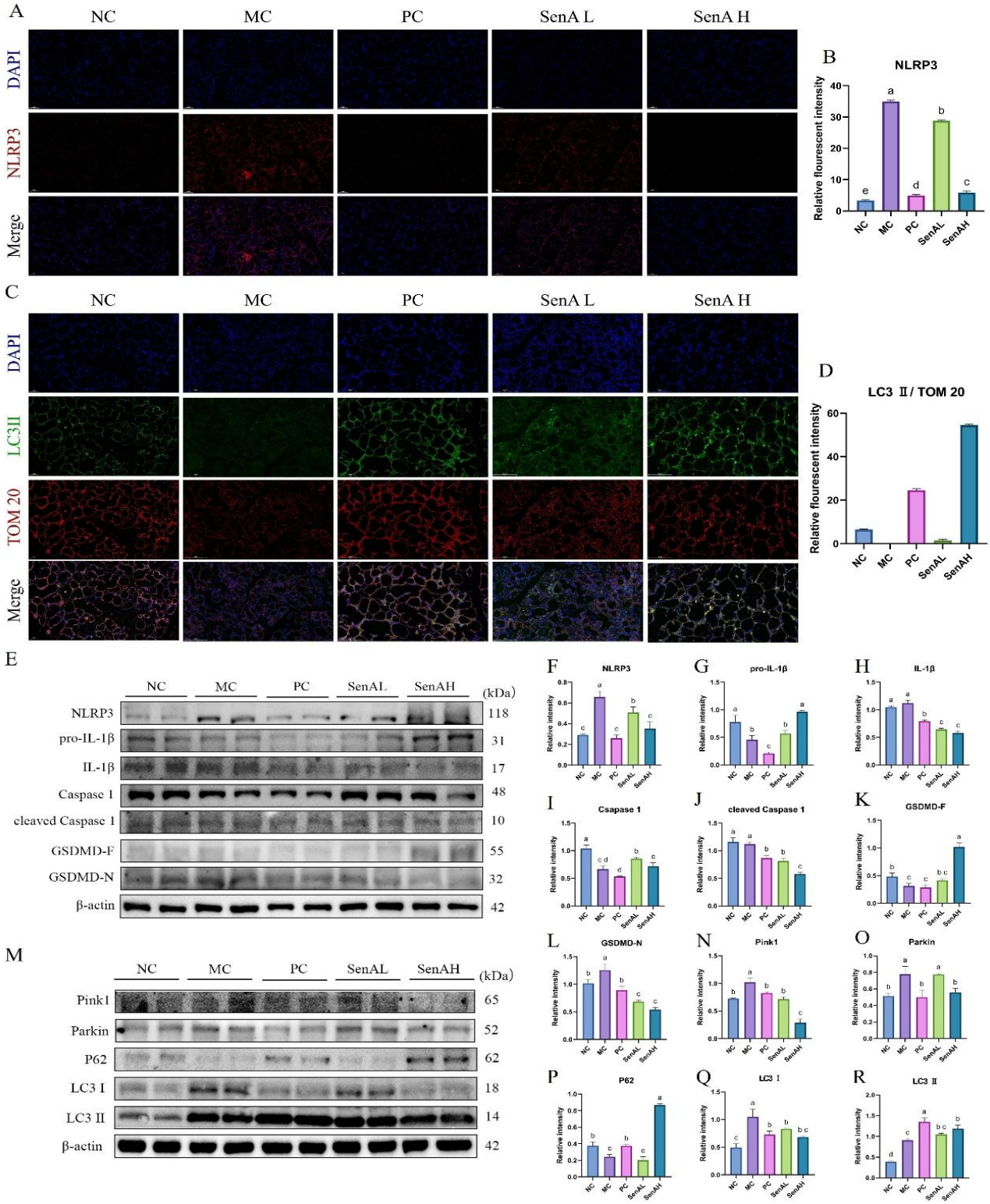


Fig. 3: SenA reduces pyroptosis-related protein processing and alters mitophagy-related responses in mammary tissue. A, Representative immunofluorescence staining of NLRP3 and DAPI. B, Quantification of NLRP3 fluorescence intensity. C, Representative immunofluorescence staining of LC3II, TOM20 and DAPI. D, Quantification of LC3II/TOM20-associated fluorescence intensity. E, Western blot analysis of NLRP3, pro-IL-1β, IL-1β, caspase-1, cleaved caspase-1, GSDMD-F and GSDMD-N. F–L, Quantification of pyroptosis-related proteins. M, Western blot analysis of PINK1, Parkin, P62, LC3 I and LC3 II. N–R, Quantification of mitophagy/autophagy-associated proteins.

SenA attenuates H_2O_2 induced injury and pyroptosis related protein processing in HC11 cells: HC11 mouse mammary epithelial cells were used to further examine the effect of SenA under oxidative stress. NLRP3 expression was increased after H_2O_2 treatment and reduced by SenA in a concentration dependent manner (Fig. 5B, $P<0.05$). Mature IL-1β was also increased by H_2O_2 and decreased after SenA treatment (Fig. 5C and D, $P<0.05$). Caspase-1 and cleaved caspase-1 were reduced by SenA, especially at 50μM (Fig. 5E and F, $P<0.05$). GSDMD-F and GSDMD-N were increased after H_2O_2 exposure and decreased after SenA treatment (Fig. 5G and H, $P<0.05$).

Mitophagy related proteins were then examined. H_2O_2 increased PINK1 and Parkin expression, whereas 50μM SenA reduced both proteins (Fig. 5J and K, $P<0.05$). P62 was decreased after H_2O_2 treatment and restored by 50μM SenA (Fig. 5L, $P<0.05$). LC3 I was increased in the H_2O_2 group and reduced after SenA treatment, whereas LC3 II was decreased by H_2O_2 and increased after SenA in a concentration dependent manner (Fig. 5M and N, $P<0.05$). These findings indicated that SenA reduced H_2O_2induced epithelial cell injury and was associated with lower pyroptosis related protein processing and altered mitophagy related responses.

H_2O_2 exposure increased ATP and LDH release compared with the control group. SenA at 25 and 50μM reduced both changes, and the effect was stronger at 50μM (Fig. 5O and P, $P<0.05$).

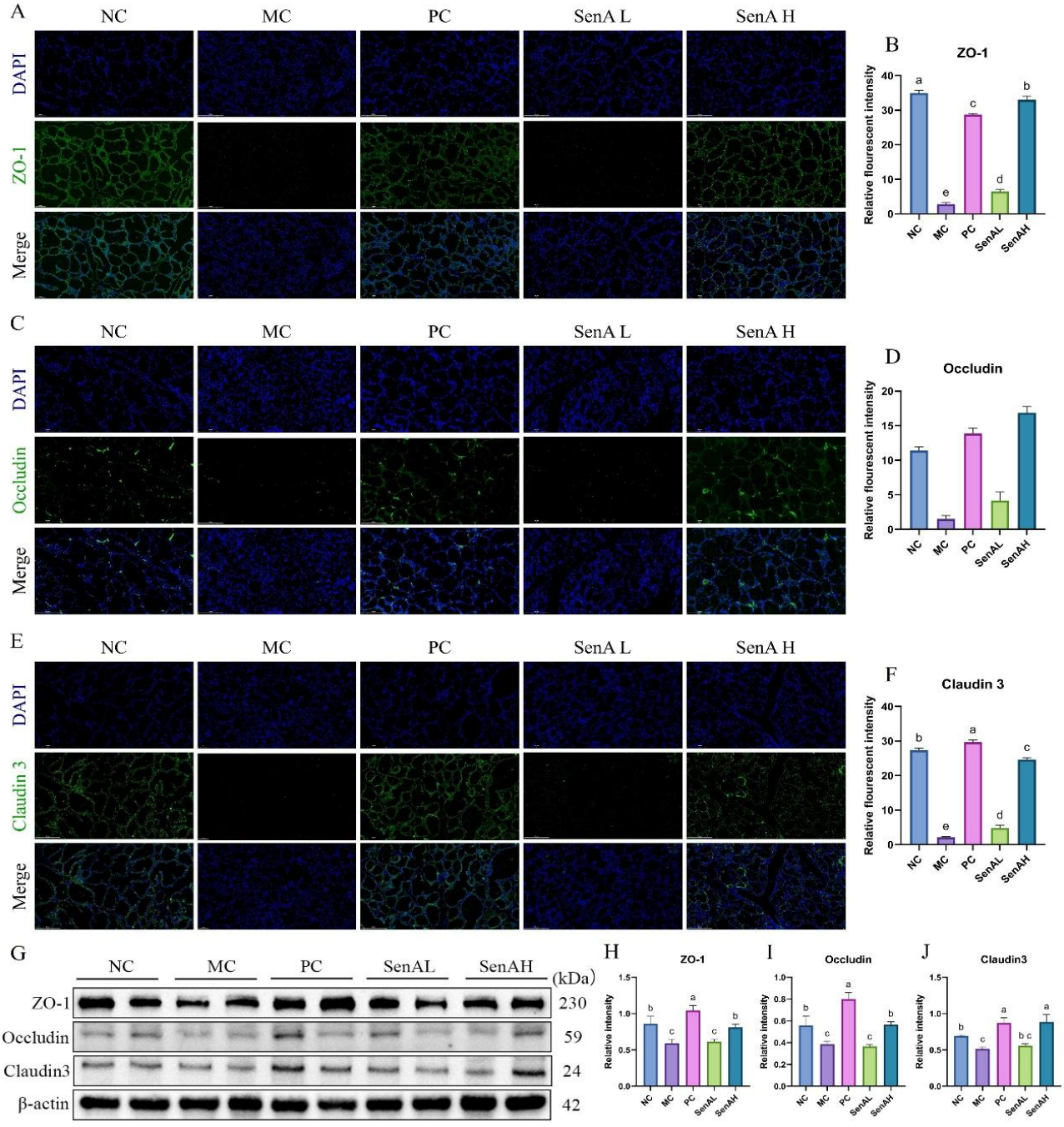


Fig. 4: SenA restores tight-junction proteins in LPS-induced murine mastitis. A, Representative immunofluorescence staining of ZO-1 and DAPI. B, Quantification of ZO-1 fluorescence intensity. C, Representative immunofluorescence staining of occludin and DAPI. D, Quantification of occludin fluorescence intensity. E, Representative immunofluorescence staining of claudin-3 and DAPI. F, Quantification of claudin-3 fluorescence intensity. G, Western blot analysis of ZO-1, occludin and claudin-3. H–J, Quantification of tight-junction proteins.

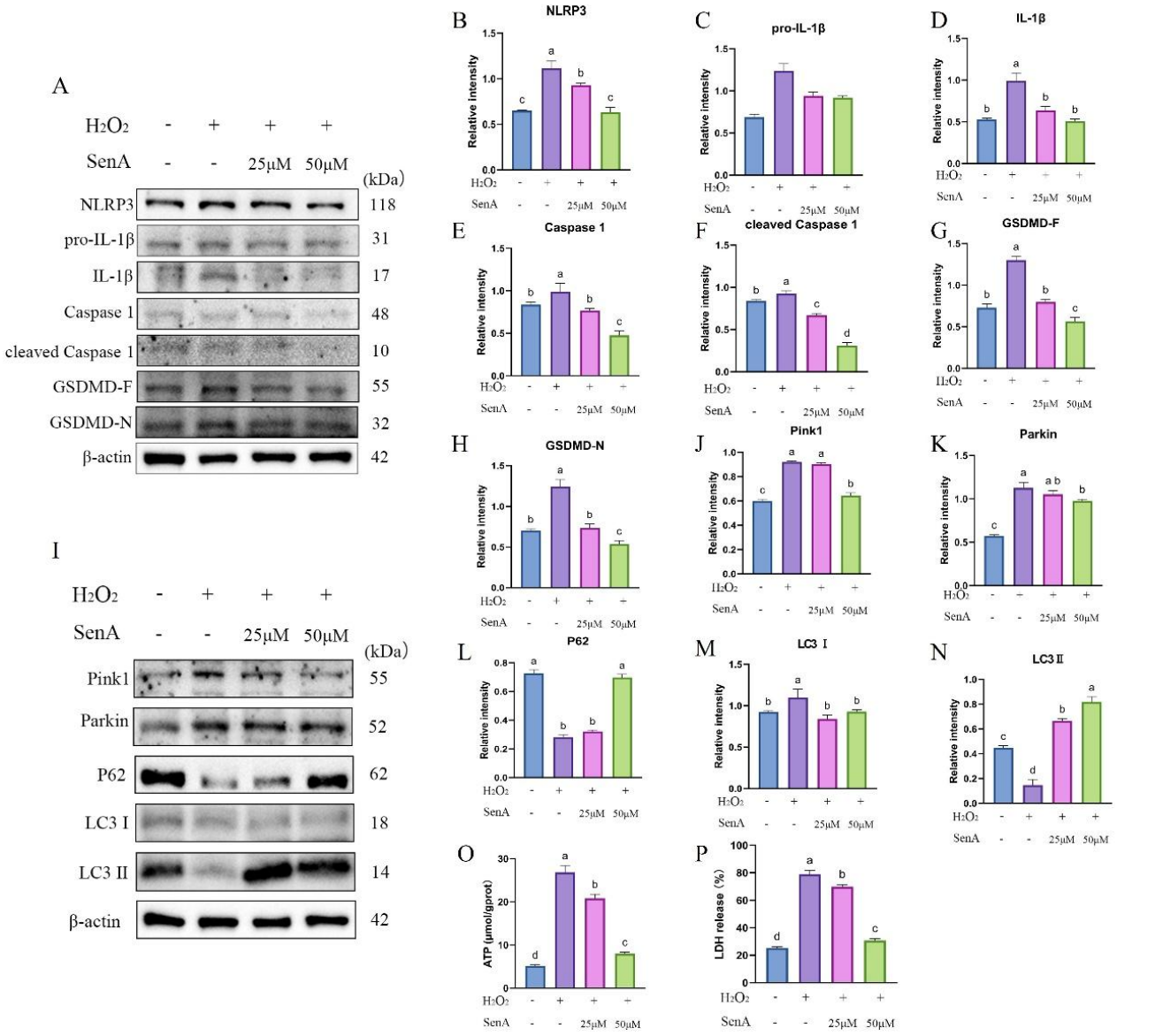


Fig. 5: SenA attenuates H_2O_2-induced injury and pyroptosis-related protein processing in HC11 cells. A, Western blot analysis of NLRP3, pro-IL-1β, IL-1β, caspase-1, cleaved caspase-1, GSDMD-F and GSDMD-N. B–H, Quantification of pyroptosis-related proteins. I, Western blot analysis of PINK1, Parkin, P62, LC3 I and LC3 II. J–N, Quantification of mitophagy/autophagy-associated proteins. O, ATP levels in cell culture supernatants. P, LDH release in cell culture supernatants.

DISCUSSION

LPS stimulation triggered severe inflammatory and oxidative imbalance in mammary tissue, with elevated pro-inflammatory IL-1β and IL-6, depleted anti-inflammatory IL-10, increased MPO and MDA and decreased antioxidant GSH and CAT (Li *et al*., 2024). Excessive inflammatory response is the core driver of aggravated mammary oedema and epithelial destruction during mastitis (Jia *et al*., 2022). Intervention with SenA, especially the high 40mg/kg dosage, reversed nearly all these disordered biochemical indicators and alleviated histopathological deterioration, indicating SenA exerts broad protective effects against multiple layers of LPS induced mammary injury.

The NLRP3 inflammasome acts as a core intracellular sensor for diverse cellular stress signals (Downs *et al*., 2020). Once activated, it triggers caspase-1 cleavage and IL-1β maturation and activated caspase-1 further cleaves full-length GSDMD to generate GSDMD-N (Zheng *et al*., 2025). This N-terminal fragment inserts into cell membranes to form pores and initiate pyroptosis, which in turn amplifies local inflammatory cascades and exacerbates mammary epithelial damage (Molina-López *et al*., 2024). Under LPS or H_2O_2 stimulation, mammary tissue and HC11 epithelial cells showed obvious upregulation of NLRP3, cleaved caspase-1, mature IL-1β and GSDMD-N (Shao *et al*., 2022). SenA robustly reversed all these abnormal molecular changes in a concentration-dependent manner across both *in-vivo* and *in-vitro* systems. Through blocking the entire inflammasome-pyroptosis signalling cascade, SenA efficiently curbs excessive inflammatory amplification within inflamed mammary glands.

Mitochondrial dysfunction acts as an upstream stimulus that links oxidative stress to NLRP3 inflammasome hyperactivation (Kang *et al*., 2018). Damaged mitochondria overproduce reactive oxygen species and release damage associated signals that facilitate inflammasome assembly, whereas mitophagy removes impaired mitochondria to suppress these pro-inflammatory stimuli (Kang *et al*., 2018; Zhang *et al*., 2024). In our study, LPS and H_2O_2 disrupted

the expression of core mitophagy proteins PINK1, Parkin, P62 and LC3, while SenA remodelled mitophagic signaling and elevated LC3II/TOM20 co-localisation signals. These results suggest mitophagy modulated mitochondrial quality control participates in SenA mediated mammary protection. Notably, our current conclusions regarding mitophagy-pyroptosis crosstalk are built upon correlative observations from static protein biomarkers and LC3-TOM20 immunofluorescence co-localization, rather than direct causal evidence. We have not performed genetic or pharmacological rescue/inhibition assays to disrupt PINK1/Parkin-dependent mitophagy and test whether the anti-pyroptotic effect of SenA is abrogated upon mitophagy blockade. Therefore, we cannot definitively establish whether enhanced mitophagy is a necessary upstream mediator for SenA-mediated NLRP3-inflammasome and pyroptosis suppression. Future mechanistic studies employing mitophagy-deficient cell models (e.g. PINK1/Parkin knockout HC11 cells) or pharmacological mitophagy inhibitors are required to dissect the causal hierarchy between mitophagy restoration and inflammasome-driven pyroptosis in mammary epithelial injury.

Mammary epithelial tight junctions serve as a critical physical partition between gland luminal and interstitial spaces, restricting the diffusion of inflammatory mediators across mammary tissue; loss of this barrier function drastically aggravates tissue damage during mastitis (Xu *et al*., 2022). The structural stability of epithelial barriers largely depends on the normal expression of core tight junction proteins including ZO-1, occludin and claudin-3. In our model, inflammatory stimulation markedly suppressed the abundance of these three proteins and destroyed epithelial compartmentalisation (Hu *et al*., 2024). As observed in both immunofluorescence and western blot assays, SenA effectively restored the expression of ZO-1, occludin and claudin-3 to recover mammary epithelial barrier integrity. This barrier-protective effect of SenA may partly stem from its suppression of pyroptosis, because pyroptosis-mediated membrane perforation and massive secretion of IL-1β work together to disrupt tight junction structure and function.

Several limitations of this research need to be addressed. First, the LPS induced mastitis model only simulates acute chemical mammary inflammation and cannot fully recapitulate the complex features of natural livestock mastitis. Second, HC11 mouse mammary epithelial cells cannot perfectly represent primary dairy cow mammary epithelium, which limits the direct translational value of our cellular data. Third, we did not conduct pathway rescue assays to confirm the causal relationship between mitophagy modulation and inflammasome inhibition. Although our data reveal a correlation between SenA treatment, mitophagy remodelling and relieved pyroptotic injury, more mechanistic validation is still necessary.

SenA mitigates LPS induced inflammatory and oxidative mammary damage, inhibits NLRP3 inflammasome dependent pyroptosis, modulates PINK1/Parkin mitophagy and restores mammary epithelial tight junction integrity. This study provides experimental support for developing SenA as a candidate agent for treating lactational mastitis.

Conclusions: In this study, SenA attenuated LPS induced murine mastitis and protected HC11 mammary epithelial cells from H_2O_2induced injury. SenA reduced inflammatory and oxidative responses, suppressed inflammasome dependent pyroptotic protein processing, modified mitophagy related mitochondrial quality control responses and helped preserve mammary epithelial barrier integrity. These findings suggest that SenA may be a promising natural immunopharmacological candidate for inflammatory mammary injury. Since our present data demonstrate correlative but not causal associations between mitophagy remodelling and pyroptosis suppression, future loss-of-function assays targeting PINK1/Parkin-dependent mitophagy are essential to clarify whether mitophagy activation is required for SenA-dependent inhibition of inflammasome-triggered pyroptosis.

Author's contribution statement: MJ, JC: Writing–review & editing, Writing–original draft, Visualization, Methodology, Conceptualization; YF, QH, JS WB: Visualization, Methodology, Conceptualization, Validation, Software, Data curation; FD: Writing–review & editing; SD, XG, WQ: Writing–review & editing, Funding acquisition, Conceptualization, Supervision, Project administration, Methodology, Funding acquisition; MK: Writing–review & editing, Funding acquisition, Conceptualization, Supervision, Formal analysis.

Funding: This work was supported by the Yunnan Major Science and Technology Special Project (Grant No. 202502AE090054), the Yunnan Key Laboratory of Veterinary Etiological Biology (Grant No. 202449CE340019) and the Deanship of Scientific Research, Vice Presidency for Graduate Studies and Scientific Research, King Faisal University, Saudi Arabia (Grant No. KFU265658).

Ethics approval and consent to participate: All animal experiments were approved by the Animal Ethics Committee of Yunnan Agricultural University (approval No. APYNAU20260730) and were performed in accordance with institutional guidelines for the care and use of laboratory animals.

Declaration of competing interest: The authors declare that they have no known competing financial interests or personal relationships that could have appeared to influence the work reported in this paper.

Data availability: Data will be made available on request.

REFERENCES

Aghamohammadi MD, Haine DF, Kelton HW, *et al*., 2018. Herd-level mastitis-associated costs on Canadian dairy farms. Frontiers in Veterinary Science 5:100.

Bao LH, Sun Y, Zhao L, *et al*., 2023. Hexadecanamide alleviates *Staphylococcus aureus*-induced mastitis in mice by inhibiting inflammatory responses and restoring blood-milk barrier integrity. PLoS Pathogens 19:e1011764.

Biswas R, Sarkar A, Alam M, *et al*.,2023. Microwave and ultrasound-assisted extraction of bioactive compounds from Papaya: A sustainable green process. Ultrasonic Sonochemistry 101:106677.

Chen LJ, Su YA, Lin TH, *et al*., 2025. Th1 Cytokines inhibit acinar morphogenesis and milk protein expression in 3D mammary cultures. Biomedicines 13(6):1455.

Downs KP, Nguyen H, Dorfleutner A, *et al*., 2020. An overview of the non-canonical inflammasome. Molecular Aspects of Medicine 76:100924.

Gonçalves JL, de Campos JL, Steinberger AJ, *et al*., 2022. Incidence and treatments of bovine mastitis and other diseases on 37 dairy farms in Wisconsin. Pathogens 11(11):1282.

Hu X, He Z, Zhao C, *et al*., 2024. Gut/rumen-mammary gland axis in mastitis: Gut/rumen microbiota-mediated "gastroenterogenic mastitis. Journal of Advanced Research 55:159-71.

Jia L, Wang J, Luoreng Z, *et al*., 2022. Progress in expression pattern and molecular regulation mechanism of LncRNA in bovine mastitis. Animals (Basel) 12(9):1059.

Kang Y, Zhang H, Zhao Y, *et al*., 2018. Telomere dysfunction disturbs macrophage mitochondrial metabolism and the NLRP3 inflammasome through the PGC-1α/TNFAIP3 axis. Cell Reports 22:3493-506.

Li Y, Cheng Z, Ma W, *et al*., 2024. Effect of exogenous melatonin on performance and mastitis in dairy cows. Veterinary Sciences 11(9):431.

Luo Y, Kong Z, Yang B, *et al*., 2023. Relationship between microflora changes and mammary lipid metabolism in dairy cows with mastitis. Animals (Basel) 13(17):2773.

Molina-López C, Hurtado-Navarro L, García CJ, *et al*., 2024. Pathogenic NLRP3 mutants form constitutively active inflammasomes resulting in immune-metabolic limitation of IL-1β production. Nature Communications 15:1096.

Shao M, Yan Y, Zhu F, *et al*., 2022. Artemisinin analog SM934 alleviates epithelial barrier dysfunction via inhibiting apoptosis and caspase-1-mediated pyroptosis in experimental colitis. Frontiers in Pharmacology 13:849014.

Sneha Sri R, Pavithra T, Vinciya T, 2025. Integrative approaches in Alzheimer's disease: evaluating the potential of traditional, complementary and integrative medicine (TCIM). Frontiers in Pharmacology 16:1561702.

Suzuki Y, Chiba S, Nishihara K, 2021. Chemerin regulates epithelial barrier function of mammary glands in dairy cows'. Animals (Basel) 11(11):3194.

Watanabe A, Maeda Y, Murakami H, *et al*., 2025. Evaluation of the therapeutic effect of levamisole on subclinical mastitis in bovine leukemia virus-infected cows classified by proviral load. Animals (Basel) 15(14):2145.

Wu YJ, Jin SJ, Chen QQ, *et al*., 2025. Endothelial neuraminidase 1 inhibition attenuates LPS-induced acute lung injury through the CXCR4 pathway. Glycoscience & Therapy 1:100008.

Xiao R, Zhou W, Peng J, *et al*., 2025. AJDW, polysaccharide from *Albizia julibrissin*, binds to PI3K and induces cell cycle arrest and ROS-mediated pancreatic cancer cell apoptosis. Glycoscience & Therapy 1: 100003.

Xiong Y, Shen T, Lou P, *et al*., 2024. Colostrum-derived extracellular vesicles: potential multifunctional nanomedicine for alleviating mastitis. Journal of Nanobiotechnology 22:627.

Xu R, Shandilya UK, Yiannikouris A, *et al*., 2022. Ochratoxin A and citrinin differentially modulate bovine mammary epithelial cell permeability and innate immune function. Toxins (Basel) 14(9):640.

Yang J, Wu N, Xiong Y, *et al*., 2025. Differences in milk microbiota between healthy cows and those with recurring Klebsiella mastitis. One Health Advances 3:33.

Zhang X, Liu Y, Liu M, *et al*., 2024. Ellagic acid supplementation ameliorates cisplatin-induced liver injury in mice by inhibiting the NF-κB pathway and activating the Nrf2/HO-1 pathway. One Health Advances 2:20.

Zhang Z, Yao Y, Yang J, *et al*., 2023. Assessment of adaptive immune responses of dairy cows with *Burkholderia contaminans*-induced mastitis. Frontiers in Microbiology 14:1099623.

Zheng XB, Wang X, Gao SQ, *et al*., 2025. NINJ1-mediated plasma membrane rupture of pyroptotic endothelial cells exacerbates blood-brain barrier destruction caused by neutrophil extracellular traps in traumatic brain injury. Cell Death Discovery 11:69.

Zhou Y, Wang D and Yan W, 2023. Treatment effects of natural products on inflammatory bowel disease *in-vivo* and their mechanisms: based on animal experiments. Nutrients 15(4):1031.